

## KINK–ANTI-KINK INTERACTIONS IN A MODIFIED SINE–GORDON MODEL

Michel PEYRARD† and David K. CAMPBELL

*Center for Nonlinear Studies and Theoretical Division, Los Alamos National Laboratory, Los Alamos, New Mexico 87545, USA*

Received 29 November 1982  
 Revised 15 April 1983

We study numerically the interactions of a kink (K) and an antikink ( $\bar{K}$ ) in a parametrically modified sine-Gordon model with potential  $V(\phi) = (1-r)^2(1-\cos\phi)/(1+r^2+2r\cos\phi)$ . As the parameter  $r$  is varied from the pure sine-Gordon case ( $r=0$ ) to values for which the model is not completely integrable ( $r \neq 0$ ), we find that a rich structure arises in the  $K\bar{K}$  collisions. For some regions of  $r$  ( $-0.20 \lesssim r < 0$ ) this structure is very similar to that observed in  $K\bar{K}$  interactions in the  $\phi^4$  model, and we show that the theory recently suggested for these collisions also applies quantitatively to the modified sine-Gordon model. In other regions of  $r$  we observe new scattering phenomena, which we present in detail numerically and discuss in a qualitative manner analytically.

### 1. Introduction

The study of solitary waves and solitons has proved both stimulating and fruitful in many areas of the natural sciences [1, 2]. In particular, in condensed matter and particle physics, a wide variety of quasi-one-dimensional problems can be modeled by Hamiltonians of the form [1–4]

$$H = \int dx \left[ \frac{1}{2} \left( \frac{\partial \phi}{\partial t} \right)^2 + \frac{1}{2} \left( \frac{\partial \phi}{\partial x} \right)^2 + V(\phi) \right], \quad (1.1)$$

which yield nonlinear Klein–Gordon equations for the field  $\phi$ :

$$\frac{\partial^2 \phi}{\partial t^2} - \frac{\partial^2 \phi}{\partial x^2} + \frac{\partial V(\phi)}{\partial \phi} = 0. \quad (1.2)$$

† Permanent address: Laboratoire d'Optique du Réseau Cristallin. Faculté des Sciences, 6 Bd. Gabriel 21100 Dijon, France.

Among the specific potentials which have been of interest are

(1) the sine-Gordon model [1–4, 5],

$$V(\phi) = 1 - \cos \phi; \quad (1.3)$$

(2) the  $\phi^4$  model [1–4, 6],

$$V(\phi) = \frac{1}{4}(\phi^2 - 1)^2; \quad (1.4)$$

(3) the double sine-Gordon model [1–4, 7],

$$V(\phi) = (1 - \cos \phi) + \lambda \left( 1 - \cos \frac{\phi}{2} \right); \quad (1.5)$$

(4) the double quadratic model [1–4, 8],

$$V(\phi) = \frac{1}{2}(|\phi| - 1)^2, \quad (1.6)$$

where  $|\phi|$  is the absolute value of the field  $\phi$ ;  
 (5) higher order polynomial models, with poten-

tials of the generic form [9]

$$V(\phi) \equiv V(\phi, n, m) \\ = \frac{\phi^2}{2} \prod_{1 \leq i \leq n} (1 - g_i^2 \phi^2) \Big/ \prod_{1 \leq j \leq m} (1 + \gamma_j \phi^2)^2, \quad (1.7)$$

where  $g_i$  and  $\gamma_j$  are constants; and (6) the parametrically modified sine-Gordon model [10],

$$V(\phi) \equiv V_{\text{PR}}(\phi; r) = \frac{(1-r)^2(1-\cos\phi)}{1+r^2+2r\cos\phi}, \quad (1.8)$$

where  $r$  is a parameter in the range  $-1 < r < +1$ .

All of these models admit solitary wave solutions – some of them [7, 9] admit several distinct types – which have been used to describe localized nonlinear excitations in real materials and model field theories. In the case of the sine-Gordon model, eq. (1.3), these solitary waves are “solitons” in the mathematical sense: when they interact, they are always scattered elastically, preserving asymptotically their shape and experiencing only a “phase shift” [1–3, 5]. This exact soliton behavior is related to the complete integrability [1–3, 5] of the sine-Gordon system. This integrability also renders multiple soliton interactions analytically tractable [2, 5] and, as a consequence, the sine-Gordon equation has been extensively studied [1–3, 5] as an idealized model of many different physical systems.

Yet, precisely because this exact soliton behavior is so delicate, in real physical systems strict solitons are unlikely to occur. In some cases, there is a physical perturbation – a defect, an impurity, or a weak coupling to another system – that destroys the complete integrability of the idealized model. In other cases, the basic models – as in eqs. (1.4)–(1.8) – are simply not integrable. In all these instances, the solitary waves in general no longer interact like strict solitons, but in collisions can be inelastically scattered, trapped into quasistable bound states, or even completely destroyed. Apart from exceptional cases which are small per-

turbations on an integrable system, these solitary wave interactions must be studied numerically. It then becomes particularly important to identify qualitative mechanisms underlying the observed interactions and then to test whether the mechanisms found in one model apply to others.

In the immediately preceding article [11] (hereafter referred to as I), the interactions of the solitary waves – conventionally called “kinks” and “antikinks” – of the  $\phi^4$  potential model [eq. (1.4)] were studied extensively, both by numerical simulations and by analytic techniques. The results of I, which builds upon many early studies [9, 12–18] indicate that the final state in such interactions is very sensitive to the initial relative velocity of the two colliding excitations [11, 14, 15, 17, 18]. In particular, in the center of mass frame in which a kink with velocity  $v_i$  collides with an antikink with velocity  $-v_i$ , there is a critical speed  $v_c$  ( $= 0.2589\dots$ ) such that for  $|v_i| > v_c$  the K and  $\bar{K}$  reflect (inelastically) from each other and escape to infinity. For most  $|v_i| < v_c$ , the K and  $\bar{K}$  form an oscillatory, decaying bound state [11–18]. But in well-defined “windows” of  $|v_i|$  below  $v_c$ , the K $\bar{K}$  reflect once, escape to finite separation, and then return to reflect once more before separating to infinity. In I, an explanation of these “two-bounce windows” in terms of a resonant energy exchange between the translational motion of the K and  $\bar{K}$  and a localized internal oscillation was proposed. The derivation of this “resonant energy exchange” theory is presented in I, to which interested readers are referred for all details. Here we simply sketch intuitively the highlights of this approach and collect the formulae essential for our later discussion.

Simply expressed, the resonant energy exchange theory views the interaction of two solitary waves in a non-integrable model as a collision of two deformable particles, having internal modes (“shape oscillations”) of excitation, and moving under the influence of a short-range potential between the pair. The phenomenon of trapping, as observed in I for  $v < v_c$ , arises from the attractive nature of the potential and from the fact that the

internal modes of the particles are excited by the collision, thus removing energy from their kinetic motion and leading to weak binding. In terms of the actual solitary waves, these internal modes correspond to any localized eigenfunctions (beyond the ever-present translational mode) that exist in the perturbation expansion around a single solitary wave. For a freely moving solitary wave, these modes (in linear theory) move with the wave and stay localized around it; in this sense they are “internal” to the solitary wave.

The interpretation of a solitary wave interaction, for  $v \lesssim v_c$ , is that the initial collision excites the internal modes of each wave, removing enough translational kinetic energy from the system that the waves are (weakly) bound by their mutual potential. Since they are bound only weakly, they retain their individual identities as they separate to a large distance, but since they are bound, they must return to collide again. Throughout the time between the first and second collisions, the energy “stored” in the internal modes is (at least roughly) conserved. Thus in the second collision, it is possible that this energy can be retransferred to the translational kinetic energy, allowing the solitary waves (with their internal modes de-excited) to escape. For this retransfer of energy to occur, the time between the first and second collision must satisfy a resonance condition. Assuming a single internal mode with frequency  $\omega_b$ , the condition is [11]

$$\omega_b T = 2n\pi + \delta, \quad (1.9)$$

where  $T$  is the time between collisions,  $n$  is an integer, and  $\delta$  is an offset phase (chosen by convention to lie between 0 and  $2\pi$ ). Thus this first level of analysis shows that for the observed resonance windows in I, the times between the first and second collisions should be determined by (1.9).

To transform this result into a prediction about the location of resonance windows as a function of the initial velocity,  $v$ , we must relate  $T$  to  $v$ . This relation can be derived in two steps. First, from simple particle mechanics, the time between col-

lisions can be calculated in terms of the binding energy,  $\epsilon$ , of the two solitary waves after the first collision. Assuming that the solitary wave potential falls off exponentially [as it will for all the eqs. (1.3)–(1.8)], the leading result for weak binding is [11]

$$T = \frac{\pi}{a} \frac{1}{\sqrt{\epsilon}}, \quad (1.10)$$

where  $a$  is the rate of exponential fall-off of the potential between the solitary waves. Note that as  $\epsilon \rightarrow 0$  (no binding),  $T \rightarrow \infty$ , as one would expect; if the waves are not trapped, there is no second interaction. Finally, based in part on heuristic arguments but primarily on the numerical data [11] one can argue that the binding energy,  $\epsilon$ , as a function of initial velocity,  $v$ , behaves as

$$\epsilon(v) = \alpha(v_c^2 - v^2), \quad (1.11)$$

where  $\alpha$  is an empirically determined constant. Since eq. (1.11) is, in part, empirical, the resonant energy exchange theory was termed “semi-phenomenological” [11].

Inserting eq. (1.11) into eq. (1.10) gives

$$T(v) = \frac{\pi}{a\sqrt{\alpha}\sqrt{v_c^2 - v^2}} \equiv \beta \times \frac{1}{\sqrt{v_c^2 - v^2}}. \quad (1.12)$$

This final equality can be independently checked numerically and consequently the constant  $\beta$  can also be derived from the numerical results. With expression (1.12) and the resonance condition (1.9) the incoming velocity corresponding to the center of the two-bound window of index  $n$  is given by the solution to

$$(v_c - v_n)^2 = \frac{\beta^2 \omega_b^2}{(2n\pi + \delta)^2}, \quad (1.13a)$$

which, for  $v_n \approx v_c$ , is well approximated by

$$v_n \approx v_c - \frac{\beta^2 \omega_b^2}{2v_c \pi^2 (2n + \delta/\pi)^2}. \quad (1.13b)$$

In the case of the  $\phi^4$  theory, the prediction of eq. (1.13) is remarkably well satisfied [11]. Further, none of the above analysis depended on the specific character of the  $\phi^4$  potential. It is thus of considerable interest to verify that these ideas do apply to other non-integrable models of the form (1.1). The modified sine-Gordon model [eq. (1.8)] is particularly well-suited for this test. First, one can move, in a controlled manner, from an integrable model ( $r = 0$ ) to strongly nonintegrable models by varying  $r$ . Second, the number of modes corresponding to localized internal oscillations around a solitary wave solution varies as a function of  $r$ . For  $r > 0$ , there are *no* such localized modes, whereas for  $r < 0$ , the number of internal modes increases without limit as  $r \rightarrow -1$ . In view of the central role played by the single internal mode in the interpretation of the  $\phi^4$  results [11], the possibility of varying the number of such modes provides a valuable test of the theoretical analysis.

Our numerical results show a very rich phenomenology for the kink-antikink collisions in the modified sine-Gordon model. “Two-bounce windows” are indeed observed for certain values of  $r$ , and the resonant energy exchange mechanism is quantitatively confirmed by the agreement of its predictions with the numerical results. For other values of  $r$ , phenomena more complicated than “two-bounce windows” are observed, and thus while the resonant energy exchange *mechanism* appears still to be operative, the details of a quantitative *theory* remain to be worked out. In this sense our results represent only a first look at what promises to be a problem of continuing interest.

The remainder of the paper is organized into five sections. Section 2 is devoted to a description of the modified sine-Gordon model with particular emphasis on the properties of small oscillations about the kink waveform. In section 3 we describe the results of numerical simulations of  $\text{K}\bar{\text{K}}$  collisions for small values of  $r$ , so that  $V_{\text{PR}}$  is “close” to the sine-Gordon theory. We interpret these results quantitatively in terms of the resonant energy exchange mechanism. In section 4 we investigate

potentials involving larger values of  $r$ . Here we find additional scattering “channels,” which involve phenomena qualitatively different from the “two-bounce windows.” We discuss these phenomena qualitatively in terms of the resonant energy exchange mechanism. Finally, in section 5 we discuss our general conclusions.

## 2. The parametrically modified sine-Gordon model

The original motivation for constructing the modified sine-Gordon potential, eq. (1.8), was to model a strictly periodic but non-sinusoidal substrate potential in quasi-one-dimensional condensed matter systems [10]. The form of this potential is plotted for several different values of  $r$  in fig. 1. As the parameter  $r$  varies in the range  $-1 < r < +1$ , the amplitude of the potential remains constant while its shape changes from sharp wells separated by flat tops ( $r < 0$ ) to wells with flat bottoms separated by sharp peaks ( $r > 0$ ). This potential admits the sine-Gordon potential as a particular case when the parameter  $r$  is zero.

If we look for solutions of the corresponding eq. (1.2) with permanent profile propagating with a velocity  $v$ ,  $\phi(x - vt) = \phi(s)$ , they can be expressed analytically in an implicit form,  $s = s(\phi)$ . Two classes of solutions are obtained, one for positive

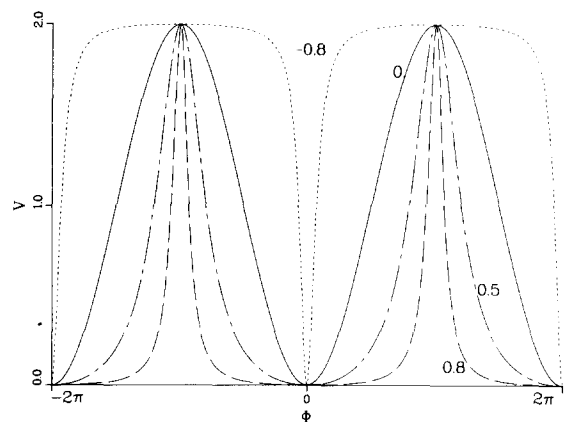


Fig. 1. Representation of the potential  $V_{\text{PR}}(\phi; r)$  for different values of the shape parameter  $r$ .

and one for negative values of  $r$ . If we define a parameter  $\rho = (1 - |r|)/(1 + |r|)$  such that  $0 < \rho < 1$ , these solutions are given by:

$0 \leq r < 1$

$$s = \frac{1}{\rho\gamma} \operatorname{sgn}(\pi - \phi) \left[ (1 - \rho^{-2})^{1/2} \tanh^{-1} \frac{(1 - \rho^2)^{1/2}}{[1 + \rho^2 \tan^2(\phi/2)]^{1/2}} - \tanh^{-1} \frac{1}{[1 + \rho^2 \tan^2(\phi/2)]^{1/2}} \right]; \quad (2.1a)$$

$-1 < r \leq 0$

$$s = \frac{\rho}{\gamma} \operatorname{sgn}(\pi - \phi) \left[ \frac{(1 - \rho^2)^{1/2}}{\rho} \tan^{-1} \frac{(1 - \rho^2)^{1/2}}{[\rho^2 + \tan^2(\phi/2)]^{1/2}} + \tanh^{-1} \frac{\rho}{[\rho^2 + \tan^2(\phi/2)]^{1/2}} \right], \quad (2.1b)$$

with  $\gamma = (1 - v^2)^{1/2}$ .

Fig. 2 illustrates that these solitary waves have a “kink-like” profile. Note that the spatial extension of the kinks increases strongly when  $r$  ap-

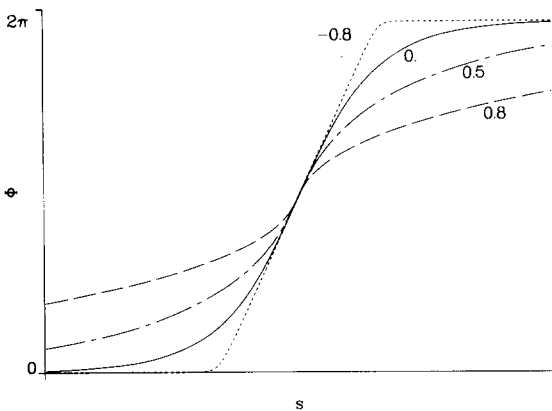


Fig. 2. Kink profile  $\phi(s)$  for various values of the shape parameter  $r$ . Note the increase of the spatial extension of the kink as  $r$  increases.

proaches  $+1$  while the kinks become very sharp when  $r$  tends to  $-1$ . These solutions are used as initial conditions in the numerical simulations of  $K\bar{K}$  collisions.

Since the small oscillations about the kink waveform are expected to play an important role in the  $K\bar{K}$  scattering process, we have computed their spectrum in this model. This is done by solving numerically the appropriate small oscillation equation,

$$\frac{\partial^2 \delta\phi}{\partial t^2} - \frac{\partial^2 \delta\phi}{\partial x^2} + \frac{\partial^2 V_{PR}}{\partial \phi^2} \Big|_{\phi_{K(R)}} \delta\phi = 0, \quad (2.2)$$

with  $V_{PR}(\phi; r)$  given by (1.8) and  $\phi_{K(R)}$  given by the numerical inversion of the implicit solutions in (2.1).

Fig. 3 shows the shape of the potential in (2.2)

$$v[\phi_{K(R)}(x)] \equiv \frac{\partial^2 V}{\partial \phi^2} [\phi_{K(R)}], \quad (2.3)$$

for different values of  $r$ . The two limiting cases of this potential as  $r \rightarrow \pm 1$  are an attractive  $\delta$  function (with two smaller repulsive lips) for  $r \rightarrow +1$  and an

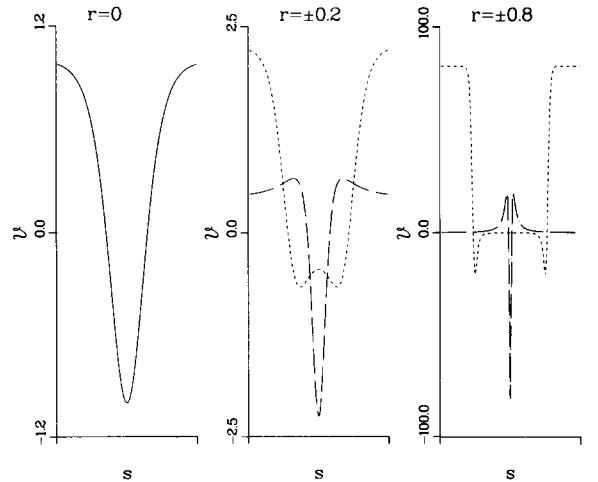


Fig. 3. Potential  $v[\phi_K(s)]$  for the small amplitude oscillations about the kink waveform for different values of  $r$ .

infinite square well (with two additional very sharp wells) for  $r \rightarrow -1$ .

Fig. 4 represents the spectrum of the small amplitude excitations as a function of  $r$ . The lower frequency of the continuum parts of the spectrum  $\omega_c = (1-r)/(1+r)$  increases from 0 to infinity as  $r$  varies from  $+1$  to  $-1$ . No bound states (except the translation mode at zero frequency) exist for positive values of  $r$ . In contrast, for negative values of  $r$  the number of bound states increases as  $r$  decreases. In the limit  $r$  tending to  $-1$  their number tends to infinity and they correspond to all integer values, as expected for an infinite square well. (For instance we have observed the 18 bound states for the value  $r = -0.9$ , corresponding to  $\omega_c = 19$ .)

The numerical method used for the simulation of  $K\bar{K}$  collisions in this model has been previously described [10]. Basically, it consists in solving with a fourth order Runge-Kutta method the New-

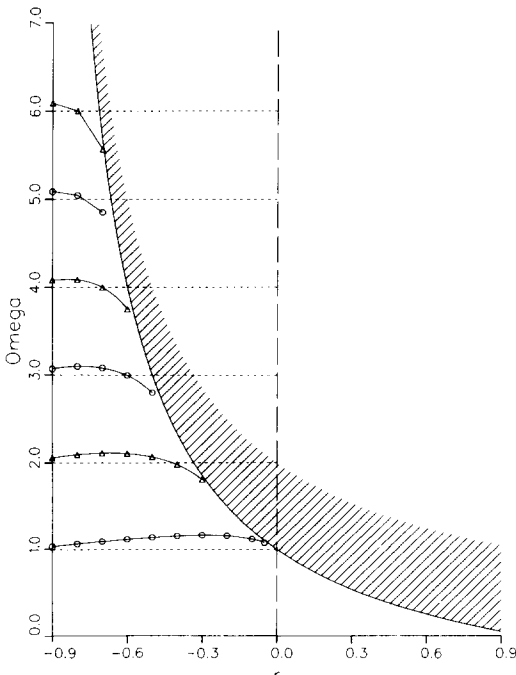


Fig. 4. Spectrum of the small amplitude oscillations about the kink waveform as a function of  $r$ . The shaded area corresponds to the continuum ( $\omega \geq \omega_c$ , non-localized states), circles indicate odd localized states and triangles even localized states.

tonian equations of motion of a discrete chain whose continuum analog is described by eq. (1.2). In such an approach, great care must be taken to avoid any discreteness effects on the kink propagation. Typically, the system studied consists of a chain of 600 particles, and the kink width is greater than 20 unit cells.

### 3. Kink-antikink scattering for small $r$

For small values of  $r$  – say  $|r| \leq 0.1$  – the  $V_{PR}(\phi; r)$  remains quite close in form to the sine-Gordon potential. Nonetheless, our earlier remarks on the delicacy of the complete integrability of the sine-Gordon system lead us to expect interesting, non-trivial  $K\bar{K}$  interactions. Further, from fig. 4 we see that for small *negative*  $r$  there is precisely one localized shape mode oscillation of the kink, whereas for *positive*  $r$  there is *no* such mode. Thus a comparison of these two cases can test the predicted critical role of this localized mode in the  $K\bar{K}$  interaction.

#### 3.1. $r = -0.1$

We start with the case in which a priori the “two-bounce” resonance theory is most likely to apply. The continuous spectrum of eq. (2.2) begins at  $\omega_c = (1-r)/(1+r) = 1.2222$  and the localized shape mode occurs at  $\omega_B = 1.1205$ . Thus we can expect that the properties of the  $K\bar{K}$  collisions in this case would be similar to those in the  $\phi^4$  model. The outgoing velocity of the kinks as a function of their incoming velocity is plotted on fig. 5. The insets to this figure show the position  $\phi_0 \equiv \phi(x=0, t)$  of the middle of the chain as a function of time for different cases. In the initial state this position ( $\phi_0 = 4\pi$ ) results from the addition of the two values  $\phi_0^K = 2\pi$  and  $\phi_0^{\bar{K}} = 2\pi$  provided by the kink and the antikink. When the two excitations pass through each other, the final value is  $\phi_0 = 0$ . (This can be easily observed on fig. 6a.)

In addition to the existence of a critical velocity  $v_c \approx 0.175 \dots$ , fig. 5 shows the presence of narrow

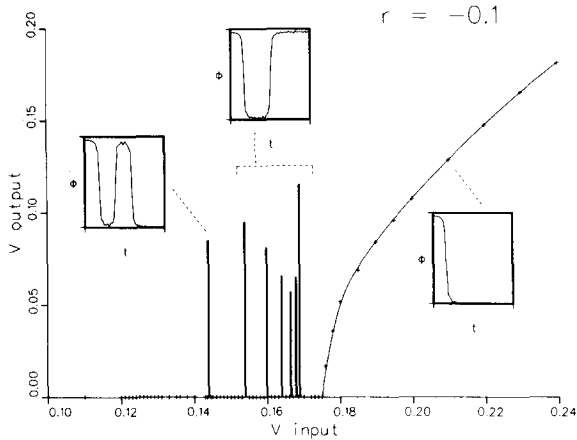


Fig. 5.  $\mathbf{K}\bar{\mathbf{K}}$  outgoing velocities as a function of their incoming velocities for  $r = -0.1$ . The bars indicating resonances of  $v < v_c$  are only schematic since these resonances are very sharp. The plots of the position of the center of the chain [ $\phi(x=0, t)$ ] as a function of  $t$  (framed pictures) show the nature of the  $\mathbf{K}\bar{\mathbf{K}}$  collisions in the different cases. Except for the resonance bars, the data points are indicated by crosses (+). On the abscissa, these appear as hash marks.

windows for  $v < v_c$  in which the kinks' outgoing velocities are non-zero. (Note however that the widths of the windows that appear in fig. 5 are not their actual widths; we discuss this below.) The diagrams which represent  $\phi_0(t)$  (and figs. 6b and c) show the exact nature of the collision in each of these windows. For the six windows with higher velocities, the scheme is rather simple: the two kinks collide and then *pass through* each other to some finite separation. This is possible here since the model is of the sine-Gordon type model – that is, has  $\phi \rightarrow \phi + 2\pi n$  symmetry – and not a double well model like the  $\phi^4$  model. Then, since the  $\mathbf{K}(\bar{\mathbf{K}})$  initial velocities are lower than the critical velocity so that the  $\mathbf{K}$  and  $\bar{\mathbf{K}}$  are trapped, they stop, come back, pass through each other a second time, and finally recede to infinity (fig. 6b). Thus the global result of the interaction of the two kinks is a *reflection* of the two excitations, as in the  $\phi^4$  model, even though the detailed interaction is slightly different because the kinks can pass through each other. Actually, it is easy to understand this behavior. Since for small  $r$  the model is quantitatively

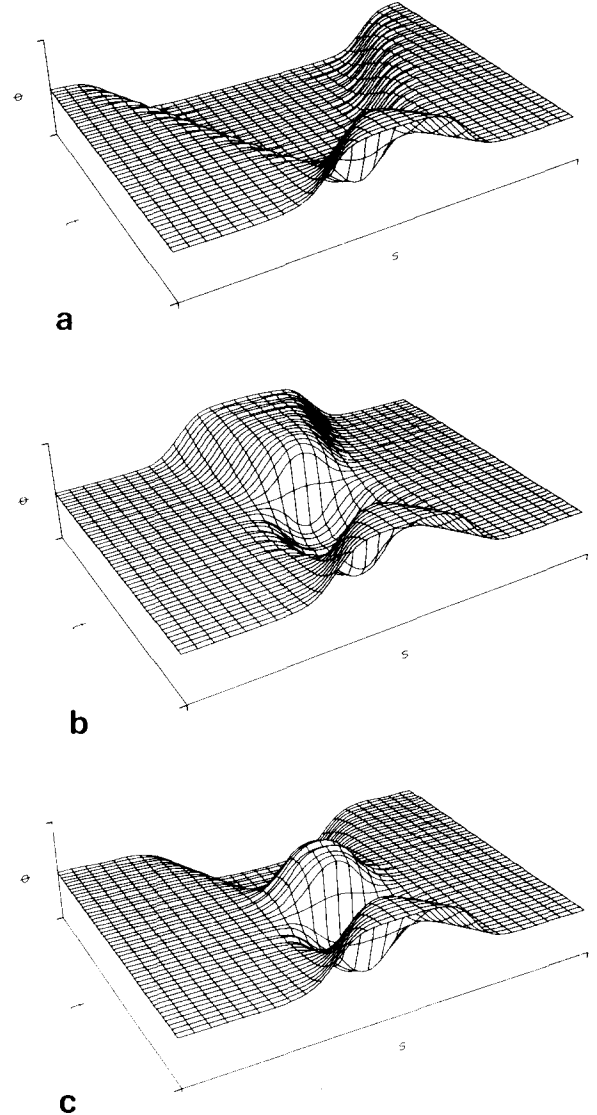


Fig. 6.  $\mathbf{K}\bar{\mathbf{K}}$  collisions for  $r = -0.1$ . a)  $v_i > v_c$  – Inelastic transmission; b)  $v_i < v_c$  – Two bounces; c)  $v_i < v_c$  – Three bounces. In all three figures, time runs “into” the projections: that is,  $t = 0$  is in the foreground and  $t = T_{\max}$  is in the background.

close to sine-Gordon, one can anticipate that the first collision of the  $\mathbf{K}\bar{\mathbf{K}}$  should not lead to reflection. If the resonant energy exchange mechanism is operative, the collision can for  $v < v_c$ , lead to trapping of the  $\mathbf{K}\bar{\mathbf{K}}$  with the lost kinetic energy primarily “stored” in the shape mode oscillation. Since they are trapped, the  $\mathbf{K}$  and  $\bar{\mathbf{K}}$  return to

interact again, but heading in the direction opposite their initial velocity. If the resonance condition (1.9) is met, the “stored” energy is retransferred to the translational motion and the kinks escape by passing through each other. Thus the overall result of a “two-bounce” interaction is quite naturally reflection.

Actually, in the case of this modified sine-Gordon equation, the term “two bounce” interaction is perhaps not as appropriate as the term “two pass” interaction would be. Nonetheless, for consistency with the earlier terminology coming from  $\phi^4$  and to stress that the resonance mechanism is the same, we retain this terminology here, defining a “bounce” as the point at which the two kinks overlap so that, with our prior conventions on the initial state,  $\phi_0 = 2\pi$ . This will be important when we discover higher “bounce” interactions later. Note that all interactions involving an odd number of bounces before escape lead to transmission, whereas those involving an even number lead to reflection.

It is interesting to note that for the window with lowest velocity in fig. 5, the process is more complicated. The two kinks pass through each other, come back, pass through each other a second time, but instead of receding to infinity they come back again, pass through each other a third time and then escape to infinity. In this case in the final state each kink has moved from one side of the system to the opposite side and finally  $\phi_0$  is equal to zero. We shall return to discuss this “three-bounce” window after analyzing quantitatively the “two-bounce” structures.

The results of applying the theoretical analysis described in section 1 to our numerical data on the “two-bounce” windows are shown in table I. For each window we have determined the time  $T_1$  between the two instants the kinks go through each other. A definite position cannot be attributed to each kink at these moments but we can extrapolate the curves that give their position before and after the collision. The point where these curves cross each other is taken as the time of impact. The values of  $T_1 \times \sqrt{v_c^2 - v^2}$  which are computed for each window are constant to within 10%, which is a reasonable accuracy, at least for determining  $v_n$  theoretically. The mean value of this product determines the “experimental” value of the constant  $\beta$  in eq. (1.12):  $\beta = 2.557$ . Fig. 7 shows the values of  $\omega_B T_1 / 2\pi$  as a function of  $n$  where  $n$  is an integer

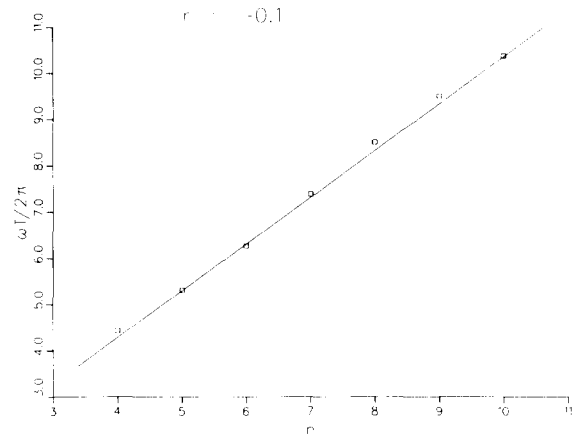


Fig. 7.  $\omega_B T_1 / 2\pi$  as a function of the window index for  $r = -0.1$ .

Table I  
Analysis of the two-bounce windows in  $K\bar{K}$  scattering for  $r = -0.1$

Center of the window: $v_n$	$v_r$	$T_1$	$T_1 \times \sqrt{v_c^2 - v_n^2}$	Index	Theoretical Value of $v_n$
0.154	0.0951	29.80	2.476	5	0.1538
0.160	0.0814	35.20	2.495	6	0.1600
0.164	0.0657	41.47	2.532	7	0.1639
0.1665	0.0570	47.77	2.573	8	0.1664
0.168	0.0653	53.40	2.617	9	0.1681
0.169	0.1156	58.30	2.648	10	0.1694

index for each window. The value  $n = 5$  for the lowest window has been chosen so that the offset phase  $\delta$  of eq. (1.9) is between 0 and  $2\pi$ . A straight line with a slope very close to 1 is a good fit for the points on fig. 7, in agreement with eq. (1.9), although there are small deviations. The value of  $\delta$  deduced from these data is  $\delta = 1.6$  ( $\delta/\pi \approx 0.5$ ). Another way to check the index  $n$  we attribute to each window is to count the number of oscillations that appear in the curves  $\phi_0(t)$  between the bounces. Limitations of computer time meant that we were able to perform this check only for one value of  $r$ , which was chosen to be  $r = -0.25$ . Thus we will discuss this below.

Given the value of  $\beta$  and the index  $n$ , we can compute the theoretical position of each window with eq. (1.13). As shown in table I these values are in remarkable agreement with the “experimental” values. In fact, this agreement is so good that after we determined a few windows (and consequently the corresponding values of  $\beta$  and  $n$ ) we were able to calculate theoretically the positions of the other ones. The numerical simulation then revealed that they were actually very close to the estimated values. This way of finding the windows actually saved considerable computation time, since the windows are quite narrow and consequently very difficult to detect.

The results presented in table I show that the theory proposed to explain the “two-bounce” windows observed in the  $\phi^4$  model can also be applied to our parametrically modified sine-Gordon model.

Several specific remarks can further illuminate our results for  $r = -0.1$ . First, in the case we study here the widths of the windows are very small and we did not attempt to determine them. According to the results on the  $\phi^4$  model, they decrease roughly as  $1/(2n)^3$ . In the case of  $r = -0.1$  the lowest “two-bounce” window ( $n = 5$ ) has a width which is less than 0.0006 units of velocity (recall we are working with dimensionless velocities). This explains why we did not make any attempt to find the widths of the other windows or to detect the windows corresponding to  $n > 10$ , for this would

have required extremely long calculations. For the case  $r = -0.25$  treated in section 4, we will present some rough determinations of window widths. For the same reason we did not attempt to study several incoming velocities inside one window. As a consequence the outgoing velocity we indicate for each window is probably *not* the maximum outgoing velocity corresponding to this window. This explains the apparent erratic behavior of the outgoing velocities as a function of  $n$  (table I) and the larger than anticipated – at least on the basis of comparable results [11] in  $\phi^4$  – inelasticity in the windows. Second, the value of  $\beta$  we used to determine “theoretically”  $v_f$  is the “experimental” value deduced from the mean value of  $T_1 \times \sqrt{v_c^2 - v^2}$ . The constant  $\beta$  can also be evaluated theoretically from eq. (1.12):  $\beta = \pi/a\sqrt{\alpha}$  with  $a = \omega_c$ . The constant  $\alpha$ , determined from the numerical data for  $v > v_c$ , is  $\alpha \approx 0.74$ , which gives a theoretical value  $\beta = 2.337$  instead of 2.577. Since this theoretical value is deduced from an approximation (valid for large separation) to the potential between the two kinks, we have calculated numerically this potential by the method described in I to check the range of validity of this approximation. The results show that an exponential approximation to the potential is valid if the distance between the two kinks is greater than 3 times their widths. The value of the constant  $a$  [in eq. (1.10)] deduced from this calculation is  $a = 1.268$ , which is close to, but not identical to, the theoretical value  $\omega_c = 1.222$  [11]. The numerical simulations show that, for the smallest value of  $n$  ( $n = 5$ ), while the kinks remain bounded by the potential (before they recede to infinity) their maximum relative distance is about 6 kink-widths and the time during which this distance is smaller than 3 kink-widths is about  $T_1/20$ , where  $T_1$  is the time between the first and second collisions. Thus the assumption, required to derive (1.10), that the kinks spend most of the time between their first two interactions in the asymptotic region, is valid. For larger values of  $n$ , we have found that this assumption is even better.

Finally, as we have indicated previously, the

nature of the  $K\bar{K}$  collision in the lowest window shown in fig. 6 is qualitatively different from the others: namely, as shown in the inset to fig. 6, it is a “three-bounce” window. Interestingly, this resonance occurs quite near to the predicted  $n = 4$  “two-bounce” window location. Specifically, for this window the numerically observed parameters are  $v_n = 0.144$ ,  $v_r = 0.0852$ , and  $T_1 = 24.85$ , where  $T_1$  is the time between the *first* two bounces shown in the inset to fig. 6. Thus if we calculate  $T_1 \times \sqrt{v_c^2 - v_n^2}$ , we find it equals 2.471, in good agreement with the corresponding quantity for the “two-bounce” windows shown in table I. Further, if we assign  $n = 4$  to the window, the theoretical value of velocity at its center is  $v_n = 0.1427$ , in reasonable agreement with the numerical result.

We have as yet no explanation of this result but are currently investigating several features related to it, including whether one can observe nearby “three-bounce” windows with the same  $T_1$ , but *different* values of the time between the second and third bounce ( $T_2$ ) corresponding to different multiples of the shape mode period. For reasons detailed in the context of higher bounce windows in the  $\phi^4$  theory [11], these putative windows are expected to be very delicate, and we have been unable to observe them. Similarly, we have been unable to observe any “two-bounce” windows – or indeed, *any* other resonances for smaller  $v$  – for  $n < 4$ . Since the quantitative aspects of the resonant energy exchange theory are expected to work only for a limited range of resonances [11] –  $n_{\min} < n < n_{\max}$  – these results are perhaps not surprising.

To summarize the results for  $r = -0.1$ , we can say that for the observed “two-bounce” windows the resonant energy exchange theory works remarkably well quantitatively and indeed was used to locate some of the very narrow, high  $n$  windows. Near the expected location of the  $n = 4$  “two-bounce” window, we found a “three-bounce” resonance, whose existence and form are qualitatively as expected from the general resonant energy exchange mechanism, but which is not yet understood in detail.

### 3.2. Small positive $r$

For small positive  $r$ , there is no localized shape mode for the kink or antikink, and hence a rigid application of the resonant energy exchange theory would suggest that *no* resonance windows should be seen below the capture threshold,  $v_c$ . On the other hand, one might be tempted to suggest an alternative possibility that, although there are strictly no modes which stay localized around the  $K$  and  $\bar{K}$ , in the initial collision a *wave packet* of continuum modes could be excited in such a way that, between the time of the first and second bounce, it did not disperse “very much” and was thus “available” at the time of the second bounce to retransfer its energy into kink kinetic energy. Our numerical results for small positive  $r$  will provide a first test to distinguish between the two possibilities.

#### 3.2.1. $r = +0.1$

For purposes of direct comparison with our previous results, we start our study of positive  $r$  with  $r = +0.1$ . In this case the kinks have slightly larger spatial extension than those of the sine-Gordon theory and thus they interact at larger distances. The limiting frequency of the small non-localized oscillations about the kink waveform is  $\omega_c = (1 - r)/(1 + r) = 0.8182$  and, importantly, no localized oscillation exists.

Fig. 8 represents the outgoing velocity of the kinks as a function of their incoming velocities. As expected we found a critical velocity  $v_c(v_c = 0.234 \dots)$  such that two kinks colliding with initial velocities  $v < v_c$  do not separate from each other but rather form a bound  $K\bar{K}$  pair. This state is unstable, and decays quickly into nonlocalized radiation which spreads over the whole system as shown on fig. 9. For  $v < v_c$  we did not find any value of the initial velocity for which the kinks escape from this bound state and recede to infinity. This result is consistent with the resonant energy exchange theory explaining the “windows” in the  $\phi^4$  model, since there is no localized state in the

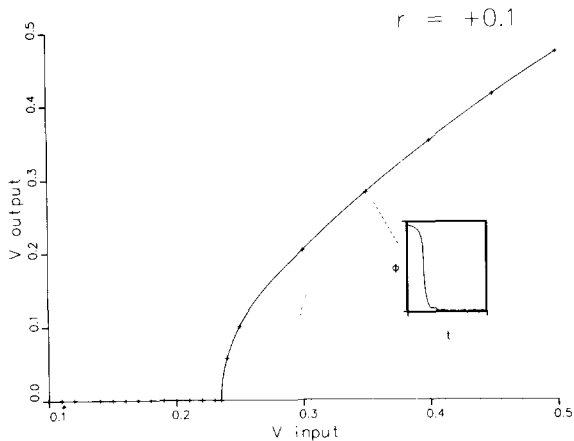


Fig. 8.  $K\bar{K}$  outgoing velocities ( $v_o$ ) after their collision as a function of their incoming velocities ( $v_i$ ) for  $r = +0.1$ . The small figure in the inset is the plot of the position on the center of the chain as a function of time.

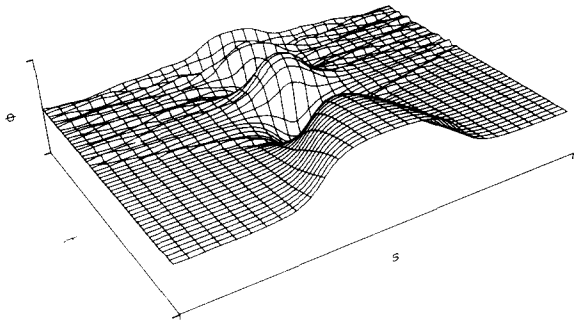


Fig. 9.  $K\bar{K}$  collision for  $r = +0.1$  and  $v_i < v_c$  ( $v_i = 0.1$ ). Note the quick spread of the energy over the whole system after the interaction due to the absence of localized states in the small oscillations.

deviations about the kink waveform which can “store” lost  $K\bar{K}$  kinetic energy.

Although no resonance windows are observed, it is nonetheless possible to check some of the assumptions made in the resonant energy exchange analysis. Thus, for example, the assumptions relating (for  $v < v_c$ ) the time interval,  $T_1$ , between the first and second  $K\bar{K}$  collisions first to  $\epsilon$ , the binding energy and then to  $v$  do *not* depend on the existence of a localized mode and thus should be valid also in this case. These assumptions imply the result shown in (1.12): namely,  $T_1(v) \times \sqrt{v_c^2 - v^2} = \beta$ ,

where  $\beta$  is a constant. Table II summarizes the numerical data testing this result for  $r = 0.1$ .

The results in table II show that the product  $T_1(v) \times \sqrt{v_c^2 - v^2}$  remains constant to good accuracy. From the data for  $v > v_c$  we can compute the value of the parameter  $\alpha$  of eq. (1.11) which enables us to deduce the binding energy of the two kinks. We obtain  $\alpha \approx 0.84$  so that the theoretical value of  $\beta$  deduced from eq. (1.12) is  $\beta = 4.18$ , which is about 20% higher than the “experimental” value.

Table II

The time,  $T_1$ , between the first two  $K\bar{K}$  collisions as a function of their incoming velocity for  $r = +0.1$

$v_i$	$T_1$	$T_1 \times \sqrt{v_c^2 - v_i^2}$
0.10	16.0	3.384
0.15	18.975	3.407
0.18	22.825	3.412
0.20	28.05	3.407

### 3.2.2. $r = +0.05$

As a further and perhaps more demanding test of the role of the localized shape oscillations, we next choose  $r = +0.05$ ; for this case the continuum begins at  $\omega_c = (1 - r)/(1 + r) = 0.9048$ . For this very small value of  $r$  the potential is very close to that of the sine-Gordon model and consequently the non-integrable effects in the  $K\bar{K}$  collisions should be very weak. This is reflected in the small value of the critical velocity,  $v_c = 0.112$ , below which kinks capture each other.

Despite a careful search (variation of the initial velocities of the kinks  $v_i$  by steps between 0.002 and 0.0002), we did not find any window of  $v_i$  for which the two excitations separate from each other for  $v_i < v_c$ . The result is in agreement with the theory relating these resonances to the existence of a bound state in the small oscillations about the kink waveform. In contrast to the case with  $r = +0.1$ , we observed here that the two kinks form a relatively stable oscillating bound state, in agreement with recent analytic calculations [19], which suggest that such stable “breathers” exist for  $r < 0.1$  for the modified sine-Gordon model.

Let us discuss these oscillating states, and in particular, their initial formation, in more detail. For  $v_i < v_c$  we denote by  $T_1$  the time between the first two collisions of the kinks and by  $T_2$  the time between the second and the third collision. The dependence of  $T_1$  and  $T_2$  upon  $v_i$  is plotted in fig. 10. The dependence of  $T_1(v)$  is well described by the familiar form,  $T_1(v) \times \sqrt{v_c^2 - v^2} = \beta$ , with  $\beta = 3.1$ . The quality of the fit is shown in table III.

Since the interaction between the kinks is rather small, they reach a rather large separation during their oscillations (typically 8 times their width) and

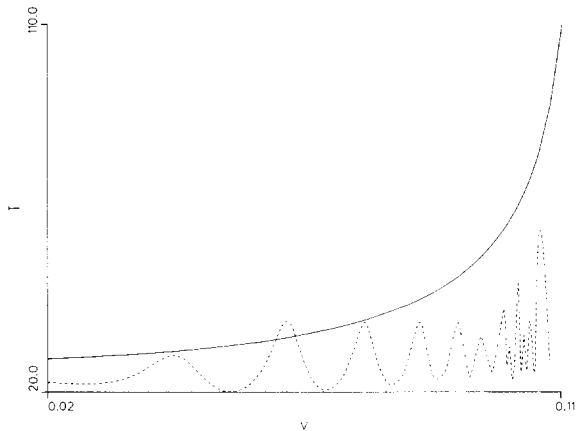


Fig. 10. The time ( $T_1$ , full line) between the first two KR collisions and the time ( $T_2$ , dashed line) between their second and third collisions as functions of their initial velocity. Both curves are smooth interpolations of the numerical data. The actual data points have been suppressed for clarity.

Table III  
Values of  $T_1$  and the product  
 $T_1 \times \sqrt{v_c^2 - v_i^2}$  for a range of  $v_i$

$v_i$	$T_1$	$T_1 \times \sqrt{v_c^2 - v_i^2}$
0.02	28.1	3.097
0.03	28.8	3.107
0.04	29.7	3.107
0.05	31.1	3.116
0.06	32.8	3.106
0.07	35.6	3.112
0.08	39.7	3.115
0.09	46.3	3.089
0.10	59.9	3.021

thus the assumptions yielding the relation between  $T_1$  and  $v$  should be valid here to a good approximation. The theoretical value of  $\beta$ , from eq. (1.12) is  $\beta = \pi/(a\sqrt{\alpha})$  with  $a = \omega_c$ . The study of  $v_f$  as a function of  $v_i$  for  $v_i > v_c$  yields  $\alpha = 1.0$  and consequently the theoretical value of  $\beta$  is  $\beta = 3.47$ , compared to the fitted value of 3.1.

The curve  $T_2(v)$  is even more interesting. Note that if some resonances were present (as in the case for negative values of  $r$ ), for some definite velocities this time should tend to infinity. This is, of course, not the case here, since as we have already indicated, no resonances are observed. However, the plot of  $T_2(v)$  in fig. 10 does show well-defined maxima. These maxima correspond to particular values of  $v_i$  for which the two excitations go rather far from each other after their second collision but do not actually separate to infinity. An example of this behavior is shown in fig. 11. Thus for  $r = +0.05$  we observe “quasi-resonances” and the corresponding initial velocities  $v_i = v_n$  are listed in the table. It is interesting to note that a formula of the type

$$v_n = v_c - \frac{A}{(2n + \delta/\pi)^2}, \quad (3.1)$$

with  $A = 5.84$  and  $\delta/\pi = 1$  gives a very good fit of the velocities of the “quasi-resonances” as listed in table IV.

It is natural to attempt to interpret the observed success of eq. (3.1) by arguing that an energy exchange mechanism similar to that that underlies the resonance window phenomena is also operating here. But instead of transferring energy to localized internal oscillations of the individual kinks, the first KR collision transfers it to a “definite” frequency,  $\omega'_c$ , in the continuum of extended states. Actually, of course, states in a range of around  $\omega'_c$  are excited; this is just the wave packet of continuum modes discussed earlier in this subsection. Since this wave packet does not correspond to a permanently localized state, during the time between the first and second collisions a substantial part of its energy spreads out away

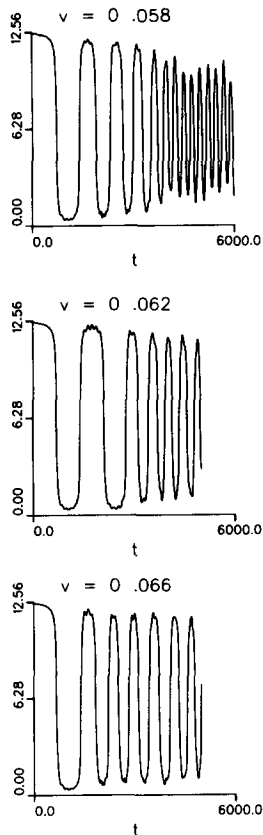


Fig. 11. The value of  $\phi(x = 0, t)$  versus  $t$  for different initial velocities near the “quasi-resonance” at  $v = 0.062$  for  $r = +0.05$ .

Table IV

The initial velocities,  $v_n$ , of the “quasi-resonances” observed for  $r = +0.05$  and the theoretical values of these  $v_n$

$v_n$	Index, $n$	Theoretical value of $v_n$
0.042	4	0.0399
0.062	5	0.0637
0.076	6	0.0774
0.085	7	0.0860
0.092	8	0.0918
0.096	9	0.0958
0.100	10	0.0987
0.101	11	0.1009
0.1025	12	0.1026
0.1035	13	0.1039
0.1045	14	0.1050
0.106	15	0.1059

from the collision center, and hence the kinks cannot recover enough energy to separate after their second collision, even though the resonance condition is satisfied. If one, by comparing (3.1) with (1.13), calculates the value of  $\omega'_c$ , one finds  $\omega'_c = 1.159$ .

This “explanation” of the “quasi-resonances” raises as many questions as it answers. For example, one would want to know what parameters determine  $\omega'_c$ , and whether it really is [as the success of (3.1) suggests] independent of the initial velocity. We are currently studying these and other questions related to the “privileged” role of localized internal oscillations.

#### 4. Kink-antikink scattering for larger $r$

When the deviation of the potential  $V_{PR}(\phi; r)$  from the cosine form increases, new channels for  $K\bar{K}$  scattering appear. The study of the positive values of the shape parameter  $r$  does not bring any qualitatively new results because no “windows” for  $v < v_c$  are observed in this case, consistent with the theoretical expectation, since no bound state exists in the small amplitude oscillations about the kink waveform. The behavior for negative values of  $r$  is thus more interesting. To give some indication of the range of the observed phenomena, we consider two cases. In the first case ( $r = -0.25$ ) only one bound state exists in the spectrum of the small amplitude oscillations and hence the situation parallels that for  $r = -0.1$  and for the  $\phi^4$  theory. In the second case ( $r = -0.5$ ), three such states exist and consequently one might anticipate somewhat different behavior.

##### 4.1. $r = -0.25$

In this case the continuum spectrum of the small amplitude oscillations begins at  $\omega_c = (1 - r)/(1 + r) = 1.6666$  and one localized state exists for  $\omega_B = 1.1675$ . The main difference from the case  $r = -0.1$  is that the ratio  $\omega_c/\omega_B$ , which is 1.090 for  $r = -0.1$ , is 1.427 and thus the energy may be

expected to be shared differently between the localized and non-localized modes in the two cases. Fig. 12 shows the outgoing velocities of the kinks as a function of their incoming velocities for this case  $r = -0.25$ . As in the case  $r = -0.1$  this figure shows very sharp peaks for  $v < v_c$  corresponding to narrow windows of  $v_i$  in which  $v_f$  is different from zero. The critical velocity is now  $v_c = 0.2925$ . It is not surprising to find a higher critical velocity than in the case  $r = -0.1$  because we are now further from the sine-Gordon case (which may be considered formally as having a zero critical velocity) and the non-integrable part of  $\text{K}\bar{\text{K}}$  interaction is correspondingly stronger.

As indicated on the insets to fig. 12, of the seven resonance windows observed, six show the familiar

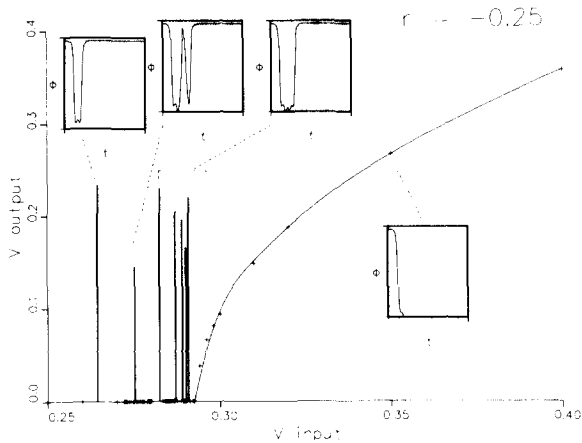


Fig. 12.  $\text{K}\bar{\text{K}}$  outgoing velocities as a function of their incoming velocities for  $r = -0.25$ .

two-bounce structure. For these one expects the resonant energy exchange theory to apply quantitatively, and thus we shall discuss these first. In table V we summarize the results of the numerical simulations and compare them with the theoretical value of the window centers.

To determine the theoretical value of the window center in table V, one needs the value of the offset phase,  $\delta$ , in eq. (1.13). As usual, we determine this by plotting  $\omega_B T_1 / 2\pi$  versus  $n$  and evaluating the intercept. The plot is shown in fig. 13. The observed values of  $\omega_B T_1 / 2\pi$  do yield, as predicted by (1.9), a relatively good straight line with slope 1. From fig. 13 and this straight line fit, one finds  $\delta = 1.7$ , so that as for  $r = -0.1$ ,  $\delta/\pi$  is close to 0.5.

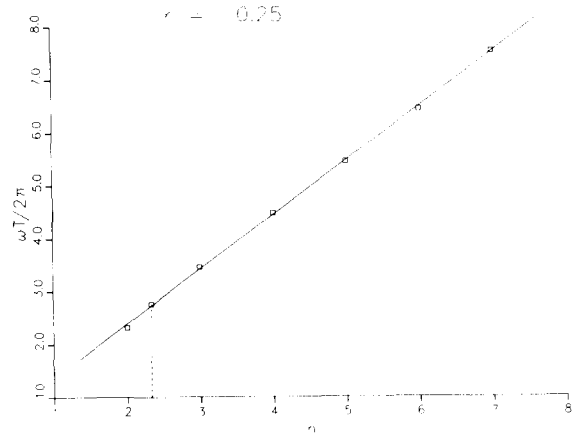


Fig. 13.  $\omega_B T_1 / 2\pi$  as a function of the window index for  $r = -0.25$ . Note the existence of a window corresponding to a non-integer value of  $n$ .

Table V

Two-bounce resonance windows in  $\text{K}\bar{\text{K}}$  scattering for  $r = -0.25$ . The detailed explanation of the data in each column is given in the text

Index, $n$	Center of the window: $v_n$	$T_1$	$T_1 \times \sqrt{v_c^2 - v_n^2}$	Theoretical value of $v_n$
2	0.2644	12.45	1.557	0.2709(0.2720)
3	0.2824	18.62	1.419	0.2821(0.2826)
4	0.2870	24.15	1.363	0.2864(0.2867)
5	0.2890	29.37	1.325	0.2885(0.2887)
6	0.2901	34.72	1.298	0.2897(0.2898)
7	0.2908	40.57	1.278	0.2904(0.2905)

For the data in table V we have an independent determination of the index of the window, which should correspond to the number of periods of the shape mode oscillation between the two collisions. In fig. 14 we show the behavior of  $\phi(x=0, t)$  for the different resonances listed in table V. One clearly sees the correspondence of the window index with the number of small oscillations of  $\phi(x=0, t)$ . It is interesting to observe that for  $r = -0.25$  the index of the lowest two-bounce window is  $n = 2$ , whereas for  $r = -0.1$ , it was  $n = 5$ . A possible explanation lies in the variation of the kink waveform as a function of  $r$ , as shown in fig. 2. For  $r = -0.25$  the kinks are significantly sharper than in the case  $r = -0.1$ , so that we might expect their interaction to be more abrupt. A

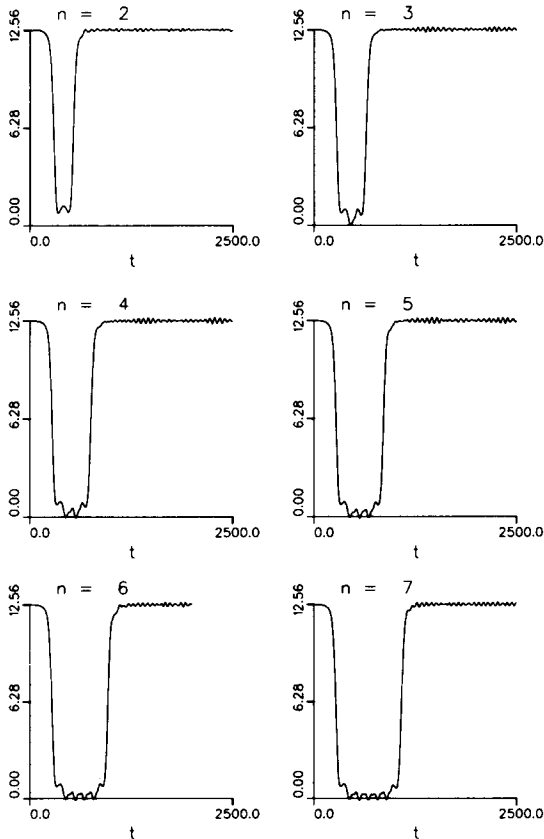


Fig. 14. The behavior of  $\phi(x=0, t)$  versus  $t$  for different initial velocities at the centers of the windows of index  $n$ , as shown, for  $r = -0.25$ .

possible consequence is that the shape modes are excited more abruptly and thus that well-defined resonances can continue to smaller  $T_1$  and have lower  $n$ .

The final factor is determining the theoretical value of the velocity at the window centers is the (supposed) constant  $\beta \equiv T_1 \times \sqrt{v_c^2 - v^2}$ . As we see from table V, the product ranges from 1.557 to 1.277 over the six windows and hence is constant only to roughly 20%. If one nonetheless defines a mean value for all six windows of  $\beta \equiv \beta_6 = 1.373$ , one obtains for velocities at the window centers the value listed in the sixth column of table V.

The observed variation in  $\beta$  must reflect the inadequacy of some of the assumptions underlying the resonant energy exchange theory. If one notices that the variation of  $\beta$  among the last five windows is considerably smaller ( $\approx 10\%$ ) than the variation ( $\approx 20\%$ ) over all six, one is naturally led to look for an explanation that focusses on this lowest window. For this window, the time between  $\mathbf{K}\bar{\mathbf{K}}$  collision is shortest and the kinks spend the least time in the region where the asymptotic form of their interaction potential is valid. Hence both the general asymptotic estimate of the time between collisions and, in particular, the very weak binding limit in (1.10) are quite likely to be inadequate. Thus it is not surprising that one sees a deviation from the assumed constancy of  $\beta$ . Note that if one uses only the last five two-bounce windows to determine  $\beta$ , one finds  $\beta \equiv \beta_5 = 1.337$ , which leads to the theoretical values of the velocities at the window centers shown in parentheses in table V.

In the discussion thus far of the case  $r = -0.25$  we have used two "experimental" values of  $\beta$ , as determined by averaging the value of  $T_1 \times \sqrt{v_c^2 - v^2}$  observed numerically. It is very interesting to compare either of these values ( $\beta_5 = 1.337$  or  $\beta_6 = 1.373$ ) to the theoretically predicted value, based on eq. (1.12). A fit of velocity data for  $v > v_c$  yields  $\alpha = 0.514$ , which given that  $a$  in (1.12) should satisfy  $a \equiv \omega_c = 1.66$ , yields a theoretical value of  $\beta$  of  $\beta = 2.629$ . Consequently, the agreement between the theoretical and "experimental" values is now quite bad. To test possible

origins of this discrepancy, we first calculated numerically the  $K\bar{K}$  potential and found good agreement with the expected exponential asymptotic form,

$$U(y) \simeq c e^{-2\alpha|y|}, \quad (4.1)$$

where  $2|y|$  is the separation between the kinks and  $c$  is a constant, provided that  $2|y|$  is greater than three times the kink width. The numerical value of  $a$  was  $a_{\text{exp}} = 1.683$ , in good agreement with the theoretical value  $a_{\text{thy}} = 1.666$ . In the worst case ( $n = 2$ ), the maximum  $K\bar{K}$  separation between bounce is  $2y_{\text{max}} = 4.5$ , and thus, as discussed above, the asymptotic estimates should at best be only marginal. But for higher  $n$ , these estimates should become more accurate, whereas the discrepancy between the theoretical and “experimental” values of  $\beta$  remains. We have been unable to identify the source of this discrepancy but the structure of eq. (1.12) suggests that it must come from one of – or perhaps a combination of – two sources. First, the semi-phenomenological relation between the binding energy  $\epsilon$  (for  $v < v_c$ ) and the final velocity (for  $v > v_c$ ) may be less accurate than in the previous cases. Second,  $U(y)$  as determined by substituting the Ansatz solution  $\phi = \phi_K(x - y) + \phi_{\bar{K}}(x + y)$  into the Hamiltonian, may in fact be a poor description of the actual “potential” involved in the  $K\bar{K}$  interaction. We are currently studying these possibilities further. Note that despite this worrying discrepancy in the theoretical value of  $\beta$ , the resonant energy exchange *mechanism* for these two-bounce collisions seems clearly established (recall fig. 14) and, if  $\beta$  is determined phenom-

enologically, the detailed *theory* works fairly well quantitatively.

To this point we have said nothing about the widths of the two-bounce resonance windows. Since the resonant energy exchange theory predicts these should be proportional to  $1/n^3$ , where  $n$  is the index of the window, it is clear that the current case of  $r = -0.25$ , in which the lowest observed window has  $n = 2$ , is much better suited to test this prediction than the previous case of  $r = -0.1$ , for which  $n_{\text{min}} = 5$ . In table VI we list our approximate determinations of the widths of the lowest three two-bounce windows for  $r = -0.25$ .

To within the (considerable) numerical uncertainties, the window widths are consistent with the anticipated scaling with  $n$ .

Our final comments on the data for  $r = -0.25$  concern the one window (at  $v = 0.2752$ ) in fig. 12 which is *not* a two-bounce window. This is shown clearly on the inset to fig. 12 and is reflected in the non-integer index,  $n = 2.33$  (see fig. 13), that arises if one attempts to fit this to the two-bounce resonance theory. The inset to fig. 12 shows that this window is in fact a “four-bounce” window, in that the kinks escape to infinity only after *four* collisions. Note that the final result of this collision is *reflection*, as for the two-bounce windows. Interestingly, the time,  $T_1$  between the first two bounces satisfies the relation  $T_1 \times \sqrt{v_c^2 - v^2} = 1.474$  with roughly the same value of  $\beta$  as for the two-bounce windows. The times  $T_2$  and  $T_3$  between the other bounces (2–3 and 3–4, respectively) are significantly smaller than  $T_1$  and in fact are roughly equal to the initial periods seen in the (permanently captured)  $K\bar{K}$  bound states formed for initial

Table VI  
Rough determination of window width for the lowest three resonance windows for  $r = -0.25$

Index, $n$	Width of window, $W$ in velocity	Product, $W \times n^3$
2	$0.0029 \pm 0.004$	$0.0200 < W \times n^3 < 0.0264$
3	$0.0010 \pm 0.0002$	$0.0216 < W \times n^3 < 0.0324$
4	$0.0006 \pm 0.0002$	$0.0256 < W \times n^3 < 0.0512$

velocities just outside the window. Note also that the data in fig. 12 suggest that this four-bounce collision is considerably less elastic than the two-bounce windows. Since each collision is to some extent inelastic, this result is intuitively appealing.

Comparing the data for  $r = -0.1$  and  $r = -0.25$ , one is struck by the existence in each case of an isolated “anomalous” resonance among the (by now familiar) two-bounce windows. Although the narrowness of any of the windows implies that other “anomalous” resonances could easily have been missed by our simulations, it is nonetheless clearly of interest to follow the evolution of the known resonance patterns as  $r$  is varied from  $r = -0.1$  to  $r = -0.25$ . At present, limitations of computer time have prevented us from carrying out the investigation. We plan to study this point in future simulations.

#### 4.2. $r = -0.5$

To investigate the effects of multiple localized internal modes of the kinks, we have studied the case  $r = -0.5$ , for which we see from fig. 4 that three such modes exist. For  $r = -0.5$  the continuum begins at  $\omega_c = (1 - r)/(1 + r) = 3.000$  and the three localized states occur at  $\omega_{B_1} = 1.1404$  (odd spatial symmetry),  $\omega_{B_2} = 2.0667$  (even spatial symmetry), and  $\omega_{B_3} = 2.7982$  (odd spatial symmetry). Fig. 15 shows the final kink velocity as a function of the initial velocity. The critical velocity is  $v_c = 0.337$ .

The results in fig. 15 are quite different from those observed for  $r = -0.1$  or  $-0.25$ . There are two sharp peaks at  $v_i = 0.315$  and  $v_i = 0.317$ , but as the insets show, neither corresponds to a two-bounce resonance. But the most striking feature of fig. 15 is the broad band in the region  $0.176 \leq v_i \leq 0.278$  in which apparently for all initial velocities the final velocities are non-zero. Of course, given the finite resolution of our set of initial velocities (indicated by the crosses on fig. 15), it is possible that this broad band consists of several separate smaller windows. This possibility is rendered somewhat unlikely by the observation

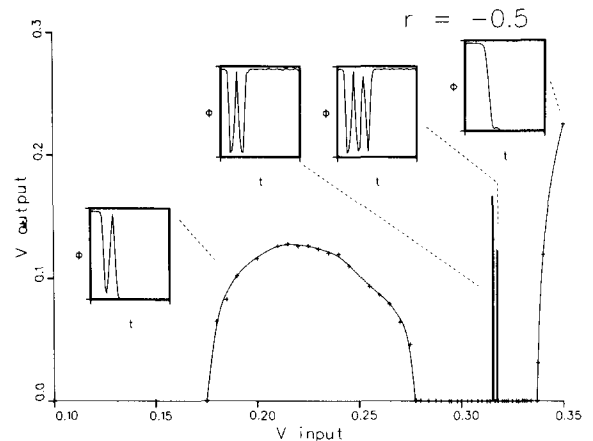


Fig. 15.  $K\bar{K}$  outgoing velocities as a function of their incoming velocities for  $r = -0.5$ .

that the collision mechanism, as indicated by inset to fig. 15, is the same for all velocities measured in this window. This mechanism involves three bounces and hence leads to transmission of  $K$  and  $\bar{K}$  through each other. Although it involves three bounces, this broad window is clearly different in structure from the three-bounce window seen for  $r = -0.1$ . In particular, the time between the bounces is relatively short –  $T_1$  varies from 7.12 for  $v_i = 0.180$  to 9.5 for  $v_i = 0.317$  – and the kinks never separate to “asymptotic” distances between collisions. For example, for  $v_i = 0.275$ , the maximum value of  $y$  between  $K\bar{K}$  collisions is only twice the kink width, and for all lower  $v_i$  inside the broad band, the maximum  $y$  is even less.

The collision mechanisms for the two higher windows also involve short intercollision times and small  $K\bar{K}$  separations. These are presumably sensitive to the short range part of the  $K\bar{K}$  interaction, and in any case the asymptotic estimates of the two-bounce theory are simply not valid. Nonetheless, comparing the two windows – the lower involving four bounces and the upper six – certainly suggests that a resonance mechanism is operating. We have searched in the vicinity of the windows for eight-bounce and two-bounce reflections – as well as for odd-bounce transmission windows – without success. In the absence of

further, more detailed information, and in the face of the wide range of a priori resonances involving the three localized modes, we have not attempted a theoretical interpretation. This clearly remains an interesting open problem. One final intriguing point arises by comparing the four-bounce window for  $r = -0.5$  with the (related?) four-bounce window observed at  $v_1 = 0.2752$  in the case  $r = -0.25$ . Despite differences, the resemblance – including the relatively low elasticity – is striking. Obviously, one again needs systematic studies of the evolution with  $r$  of the resonance patterns to unravel the mechanisms beyond the two-bounce resonance theory.

## 5. Discussion and conclusions

Since each of the preceding subsections has contained substantial discussion and analysis, in this section we shall simply summarize briefly the main qualitative conclusions and indicate a number of directions for future work.

In the cases where the two-bounce resonant energy exchange theory is applicable, it seems to work remarkably well, at least at the phenomenological level in which the crucial constants are determined empirically. The absence of resonance structure for positive  $r$  correlates strikingly with the absence of a localized shape oscillations for the kinks in this regime. This result demands more rigorous investigation [20]. The two-bounce theory, however, by no means explains all the observed phenomena, and from the results for  $r = -0.25$  and  $r = -0.5$  one sees that a possibly different mechanism, involving perhaps the more detailed, short range part of the  $K\bar{K}$  interaction, may be at work. In any event, there is clearly a need for substantial further numerical work, including systematic studies of the evolution of the resonance pattern as a function of  $r$ . Of particular interest will be the changes as the number of localized modes varies from one to two to three.

Theoretically, there are a number of obvious open problems, including analytic estimates based

on sine-Gordon perturbation theory for small  $r$  and more specifically uniform estimates for the critical velocity,  $v_c$ , as a function of  $r$ . It appears that we have only scratched the surface of the fascinating and complex subject of interaction of nonlinear excitations in non-integrable theories.

## Acknowledgements

We are grateful to our colleagues, M. Re-moissonet, J. Schonfeld, and C. Wingate, for their roles in stimulating this work. One of us (M. P.) wishes to thank the Center for Nonlinear Studies at Los Alamos for its hospitality.

## References

- [1] For a variety of recent reviews, see, for example Solitons in Condensed Matter Physics, A.R. Bishop and T. Schneider, eds. (Springer, Berlin, 1978). Physics in One Dimension, J. Bernesconi and T. Schneider, eds. (Springer, Berlin, 1981). Solitons in Action, K. Lonngren and A.C. Scott, eds. (Academic Press, New York, 1978). Solitons, R.K. Bullough and P. J. Caudrey, vol. 17 in Topics in Current Physics (Springer, Berlin, 1980), Physica Scripta 20 (1979) 291–562.
- [2] The classic introductory review is A.C. Scott, F.Y.F. Chu and D.W. McLaughlin, Proc. IEEE 61 (1973) 1443.
- [3] For reviews in the area of particle physics see, for example, S. Coleman, in: New Phenomena in Subnuclear Physics, A. Zichichi, ed. (Plenum Press, New York 1977). A. Neveu, Rep. Prog. Phys. 40 (1977) 709. R. Rajaraman, Phys. Rep. 21 (1975) 229. For a review of condensed matter applications see A.R. Bishop, J.A. Krumhansl and S.E. Trullinger, Physica D 1 (1980) 1.
- [4] R.M. DeLeonardis and S.E. Trullinger, Phys. Rev. B 22 (1980) 4558. J.F. Currie, J.A. Krumhansl, A.R. Bishop and S.E. Trullinger, Phys. Rev. B 22 (1980) 477.
- [5] J.K. Perring and T.H.R. Skyrme, Nucl. Phys. 31 (1962) 550. A. Seeger and A. Kochendörfer, Z. Phys. 130 (1951) 321. M.J. Ablowitz, D.J. Kaup, A.C. Newell and H. Segur, Phys. Rev. Lett. 31 (1973) 125. L.A. Takhtadzhyan and L.D. Faddeev, Teor. Mat. Fiz. 21 (1974) 160.
- [6] S. Aubry and R. Pick, Ferroelectrics 8 (1974) 471. J.A. Krumhansl and J.R. Schrieffer, Phys. Rev. B 11 (1975) 3535. C. Varma, Phys. Rev. B 14 (1976) 244. T. Schneider and E. Stoll, Phys. Rev. Lett. 35 (1975) 296. T. Koehler, A.R. Bishop, J.A. Krumhansl and J.R. Schrieffer, Solid State Commun. 17 (1975) 1515. Y. Wada and J.R. Schrieffer, Phys. Rev. B 18 (1978) 3897.

- G.F. Mazenko and P.S. Sahni, *Phys. Rev. B* 18 (1978) 6139; *B* 20 (1979) 4676. M. J. Rice, *Phy. Lett.* 71A (1979) 152.
- [7] K. Maki and P. Kumar, *Phys. Rev. B* 14 (1976) 3920. A.L. Mason, in: *Nonlinear Equations in Physics and Mathematics*, A.O. Barut, ed. (Reidel, Dordrecht, 1978), p. 205. P.W. Kitchenside, P.J. Caudrey and R.K. Bullough, *Physica Scripta* 20 (1979) 673. J. Shiefman and P. Kumar, *Physica Scripta* 20 (1979) 435; P. Kumar and R.R. Holland, in: *Nonlinear Problems: Present and Future*, A. Bishop, D. Campbell and B. Nicolaenko, eds. (North-Holland, Amsterdam, 1982), p. 229.
- [8] S.E. Trullinger and R.M. DeLeonardis, *Phys. Rev. A* 20 (1979) 2225.
- [9] V.G. Makhankov, *Phys. Rep.* 35C (1978) 1.
- [10] M. Remoissenet and M. Peyrard, *J. Phys. C* 14 (1981) L481; M. Peyrard and M. Remoissenet, *Phys. Rev. B* 26 (1982) 2886.
- [11] D.K. Campbell, J.F. Schonfeld and C.A. Wingate, *Physica* 9D (1983) 1 (previous paper).
- [12] A.E. Kudryavtsev, *JETP Lett.* 22 (1975) 82.
- [13] B.S. Getmanov, *JETP Lett.* 24 (1976) 291.
- [14] C.A. Wingate, Ph.D. Thesis, University of Illinois (1978) and *SIAM Journ. Appl. Math.* 43 (1983) 120.
- [15] M.J. Ablowitz, M.D. Kruskal and J.F. Ladik, *SIAM Journ. Appl. Math.* 36 (1979) 478.
- [16] T. Sugiyama, *Prog. Theor. Phys.* 61 (1979) 1550.
- [17] R. Klein, W. Hasenfratz, N. Theodorakopoulos and W. Wunderlich, *Ferroelectrics* 26 (1980) 721.
- [18] M. Moshir, *Nuc. Phys. B* 185 (1981) 318.
- [19] M. Remoissenet, private communication.
- [20] Such investigations are already in progress, specifically in the context of  $\phi^4$  theory. David McLaughlin and Harvey Segur, private communications.